THE JOURNAL OF PHYSICAL CHEMISTRY B

ARTICLE

pubs.acs.org/JPCB

Quantum Mechanical/Molecular Mechanical Molecular Dynamics and Free Energy Simulations of the Thiopurine *S*-Methyltransferase Reaction with 6-Mercaptopurine

Xiao-Liang Pan, Feng-Chao Cui, and Jing-Yao Liu*

State Key Laboratory of Theoretical and Computational Chemistry, Institute of Theoretical Chemistry, Jilin University, Changchun 130023, China

ABSTRACT: Quantum mechanical/molecular mechanical (QM/MM) molecular dynamics simulations were performed to investigate the methylation of 6-mercaptopurine catalyzed by thiopurine *S*-methyltransferase. Several setups with different tautomeric forms and orientations of the substrate were considered. It is found that, with the orientation in chain A of the X-ray structure, the substrate can form an ideal near-attack configuration for the methylation reaction, which may take place after the deprotonation of the substrate by the conserved residue Asp23 through a water chain. The potential of mean force (PMF) of the methyl-transfer step for the most favorable pathway is 19.6 kcal/mol, which is in good agreement with the available experimental rate constant data.

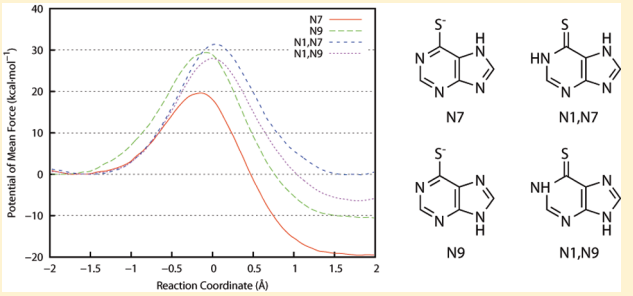

INTRODUCTION

Thiopurine *S*-methyltransferase (TPMT) is a cytosolic enzyme which is responsible for the metabolism of thiopurine and thiopyrimidine. The methylation reaction catalyzed by TPMT is an important step in the modulation of cytotoxicity of thiopurine drugs, such as 6-mercaptopurine (6MP), 6-thioguanine, and azathioprine, which are used to treat childhood acute lymphoblastic leukemia, autoimmune disorders, inflammatory bowel disease, and transplant rejection.[1] The human enzyme TPMT displays considerable person-to-person variation in activity on thiopurine drugs, mainly due to genetic polymorphisms.[2] This is a major factor in the large individual variation seen qin thiopurine toxicity and therapeutic efficacy. An understanding of TPMT activity, therefore, would provide an important insight into human health implications of toxins and drugs.

TPMT is a single domain protein with a Class-I AdoMet-dependent methyltransferase (MTase) core fold.[3] Although TPMT has been well-characterized to be able to methylate thiopurine prodrug substrates, natural substrates for this enzyme have yet to be identified. According to the recent X-ray structural studies of the enzyme,[4,5] the 6MP substrate can possess two possible orientations in the complex, related by ~180° rotation perpendicular to the plane of the ring. Figure 1 shows the orientations of the mercaptopurine in the chains A and B of the X-ray structure with respect to the protein. An internal solvent channel, with two open ends on opposite sides of the enzyme, is interconnected to the substrate binding pocket. Small molecule substrates can likely diffuse into and out of the active site through this channel.

Like most (if not all) other MTases, a classic S_N2 reaction mechanism has been proposed for the methyl-transfer step. However, some detailed mechanistic questions are still unclear. First, the catalytically active protonation state, prototropic tautomer, or binding orientation of 6MP cannot be identified from the static pictures of the crystal substructures. Second, according to the mTPMT ternary structure, there is no good candidate of solvent molecules or residues for the deprotonation of the substrate, which is required for the methyl-transfer reaction, by general acid−base catalysis.[5] Therefore, to completely understand the catalytic process in the TPMT reaction, a theoretical investigation is very desirable to address the issues mentioned above.

Because of the flexibility and partial solvent accessibility of the 6MP binding site, a single adiabatic reaction path may not be sufficient for this study. Therefore, we carried out combined quantum mechanical/molecular mechanical (QM/MM) molecular dynamics (MD) simulations to study the *S*-methylation reaction of 6MP catalyzed by TPMT and determined the free energy profile for the methyl-transfer step using the umbrella sampling technique. Our simulations have yielded activation free energy barriers consistent with the experimental results and provided insights into the mechanism of the enzymatic catalysis in thiopurine methylation.

METHODS

The initial structure of the TPMT-AdoMet-6MP complex was build upon the X-ray structure of the TPMT enzyme with AdoHcy and the 6MP substrate (PDB code 3BGD) in 2.00 Å resolution[5] with all of the retained crystallographic water

Received: March 24, 2011
Revised: May 16, 2011
Published: May 26, 2011

dx.doi.org/10.1021/jp2027516 | *J. Phys. Chem. B* 2011, 115, 8033–8037

molecules. The enzyme-bound AdoMet was built by adding a methyl group to the AdoHcy, and hydrogen atoms were added by the PDB2PQR package[6,7] with the protonation states of side chains predicted by PROPKA.[8] The resulting complex was solvated into a periodic TIP3P rectangular water box of ~78 × 92 × 79 Å^3 with a buffer distance of 12 Å between each wall and the closest atom in each direction. Counterions were added to the system to neutralize the charge. These procedures led to a system of ~46 400 atoms for the QM/MM MD simulation.

QM/MM MD simulations with periodic boundary conditions were performed with the AMBER 10 package.[9] The whole AdoMet and 6MP molecules (Scheme 1) are chosen to be the QM subsystem, whereas the enzyme and water molecules are the MM subsystem. There is no need for a special treatment for the boundary between the QM and MM subsystems because there are no covalent bonds between the substrate or the cofactor and the enzyme. The PDDG/PM3 semiempirical method, which has been argued to yield heats of formation for compounds containing C, H, N, and O atoms with significantly improved accuracy over the standard NDDO schemes,[10,11] has been used to describe the QM subsystem, and the MM subsystem is described by the AMBER03 force field[12,13] for the enzyme and the TIP3P model[14] for the water molecules. A 12 Å cutoff was introduced for nonbonding interactions. The particle-mesh Ewald (PME) method[15,16] was employed to treat long-range electrostatic interactions, and the SHAKE algorithm[17] was used to constrain all bonds involving hydrogens within the MM subsystem. A time step of 1 fs was used. After a series of minimizations and equilibrations, a 1 ns QM/MM MD simulation was carried out.

To provide mechanistic insights into the methyl-transfer reaction catalyzed by TPMT, we have used the umbrella sampling technique to calculate the potential of mean force (PMF) along the putative reaction coordinate r which was defined as $r = d(S_\zeta - C_\varepsilon) - d(C_\varepsilon - S_\delta)$. The PMF accounts for protein fluctuation and entropic effects and is essential for a more reliable estimate of the rate constant using the transition rate theory. The starting structure was the resulting snapshot of the 1 ns QM/MM MD simulation. In each series, the reaction coordinate was harmonically restrained to a range from −2.0 to 2.0 Å (at every 0.1 Å). The force constant of the biasing potential was between 360 and 620 kcal·mol^{-1}·Å^{-2}, which resulted in simulations sampling sufficiently overlapping regions of the reaction coordinate. Each simulation consisted of 10 ps of equilibration followed by 20 ps of sampling dynamics. Each subsequent equilibration was started from the 10th ps point of the adjacent equilibration run. The reaction coordinate statistics of the various simulations were combined by umbrella integration.[18,19] Further simulations were performed to confirm the convergence of the results.

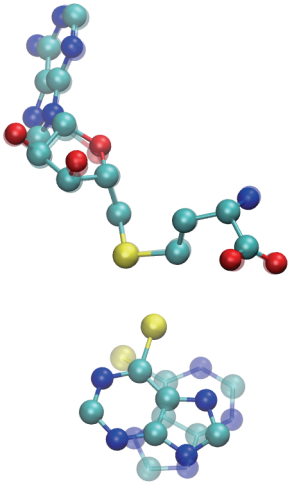

Figure 1. Superposition of the protein atoms of chains A and B of the X-ray structure with only 6MP and SAM shown.

RESULTS AND DISCUSSION

Prototropic Tautomerism and Binding Orientations of the Substrate. The prototropic tautomerism of the substrate may influence the activities, or even the mechanisms, of the catalytic reactions. In the case of 6-mercaptopurines, two types of tautomerisms might be observed (Scheme 2). One is thione−thiol equilibrium, occurring simultaneously with the proton transfer between the adjacent nitrogen and sulfur atoms (e.g., N(1)H, C(6)=S ↔ N(1)=, C(6)—SH for 6MP). If 6MP is in the thiol form, the sulfur atom should be deprotonated before attacking the methyl group of SAM, while the thione-form 6MP could, in principle, proceed without deprotonation. The other type is associated with the migration of the N-bonded mobile imine protons within the pyrimidinic (N(1)H, N(3) ↔ N(1), N(3)H) or imidazolic ring moieties (N(7)H, N(9) ↔ N(7), N(9)H). These rearrangements of the concerned π-bond aromatic system may also influence the reaction activity of the substrate. The relative energies of different tautomers of 6MP were calculated in both gas phase and continuum solvent, using the B3LYP hybrid functional[20,21] as implemented in Gaussian 09;[22] see Table 1. Overall, the tautomers with N(1)H, that is, N1,N7 and N1,N9, have predominant populations in solution. This result is consistent with the previous experimental and theoretical studies.[23,24] Besides, there are two possible binding orientations of the substrate,

Scheme 1. Methyl-Transfer Reaction Catalyzed by TPMT, in Which One Methyl Group Is Transferred from AdoMet to 6-Mercaptopurine

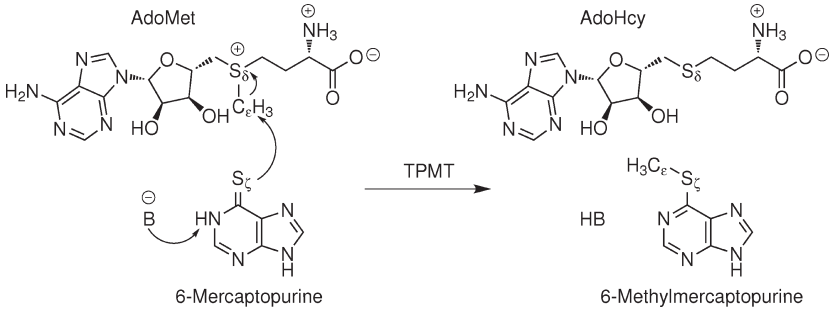

dx.doi.org/10.1021/jp2027516 |J. Phys. Chem. B 2011, 115, 8033–8037

Scheme 2. Six Possible Prototropic Tautomers of 6-Mercaptopurine

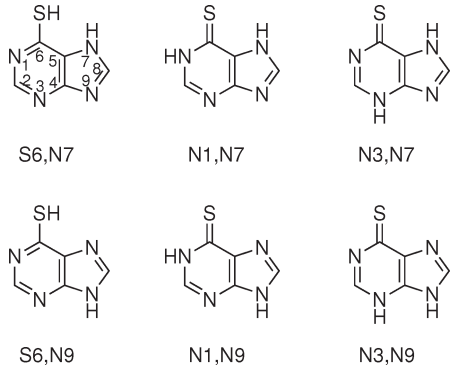

Table 1. Relative Energies of the Tautomers of 6-Mercaptopurine in kcal·mol^{-1}

	ΔE^a	ΔE(IEFPCM)^b
N1,N7	0.0	0.0
N1,N9	3.0	0.9
N3,N7	8.3	5.9
N3,N9	23.6	11.2
S6,N7	7.9	9.3
S6,N9	3.4	7.5

^{a} B3LYP/6-31+G**. ^{b} B3LYP/6-31+G**, ε = 78.3553.

as in the chains A and B of the crystal structures, respectively, and both have been considered in the following simulations.

On the basis of the discussions above, four setups of system, which differed in the prototropic tautomerism of imidazolic ring moieties and/or the binding orientations of the substrate, were built, and 1 ns QM/MM MD simulations were performed to investigate the influences of prototropic tautomerism and binding orientation on the binding stability. The distance between S_ζ and C_ε atoms, which is a good indicator for the 6MP binding stability, has been monitored and plotted in Figure 2. For the two setups built upon chain B, the distance between the transferring C_ε atom and the acceptor S_ζ atom extends to ~10 Å, suggesting that the substrate binding with the orientation as in chain B is not stable, which is consistent with the fact that a larger TPMT substrate thioinosine monophosphate (TIMP),[25] which is expected to bind similarly in the active site due to its high degree of chemical similarity to 6MP, could only fit in the orientation similar to that of 6MP in chain A.[5] The prototropic tautomerism of the substrate had no obvious influence on the binding stability.

Potential of Mean Force for Methyl-Transfer Step. Because 6MP is predominantly in the thione form, there exist two possible reaction mechanisms. On one hand, the neutral substrate can take the methyl-transfer step directly to yield a cation, and subsequently the deprotonation step could take place in the active site after the methyl-transfer step or in solvent after the release of the product; on the other hand, the deprotonated substrate has a large negative potential at S_ζ which will facilitate nucleophilic attack of the S_N2 methyl-transfer step (Figure 3), though no good candidates of solvent molecules or residues for the deprotonation of the substrate have been proposed. To model the deprotonated substrate,

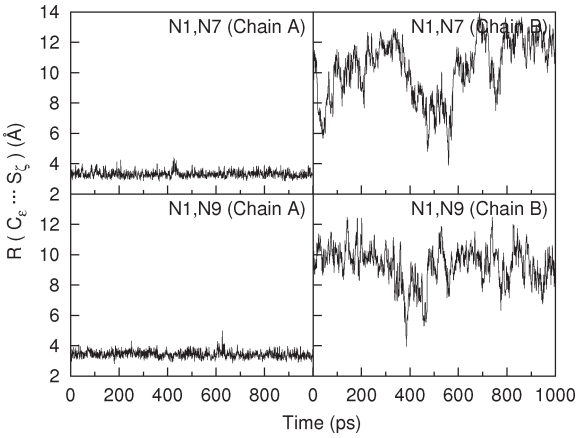

Figure 2. Time evolutions of the distance between S_ζ and C_ε atoms, which is a good indicator for the 6MP binding stability, during the 1 ns QM/MM MD simulations.

the proton attached to the N1 atom of 6MP was removed manually, and the resulting setups were processed with the procedures stated above. So far, there are four possible protonation patterns of the active substrates (Figure 3), and the substrates could be positioned in an ideal near-attack configurations (NAC) for all four setups during the 1 ns QM/MM MD simulations (Table 2).

To determine the barriers of the methyl-transfer step for the substrates with different protonation patterns, umbrella sampling simulations were performed, and the PMF for the methyl-transfer step is shown in Figure 4. The zero is arbitrarily chosen at the potential minimum corresponding to the ES complex ($r = -1.7$A). For setup N7, the calculated activation free energy barrier is 19.6 kcal/mol with a statistical error of 0.5 kcal/mol, which is in excellent agreement with the activation barrier of 20.0 kcal·mol^{-1} estimated from the experimental value of k_{cat}[5] by the simple transition state theory $k(T) = (k_B T)/h \exp(-\Delta G\ddagger/RT)$. For the other setups, the calculated activation free energy barriers are over 10 kcal·mol^{-1} higher than setup N7. Though the substrates with different protonation patterns can be positioned in a NAC in the active site of the enzyme, the relative activation barriers of the S_N2 nucleophilic attack are also influenced by the electrostatic potential at the S_ζ position of 6MP. The averaged Mulliken charges of S_ζ atom of 6MP along the reaction coordinate is plotted in Figure 5. Overall, S_ζ position of setup N7 has the most negative potential, so the methyl-transfer reaction should have the lowest activation free energy barrier, consistent with the umbrella sampling results. So we conclude that N7 is the active tautomeric form of the 6MP substrate. It should be noted that it has been proposed that 6-methylthiopurine exists predominantly as the N9 tautomer in solution.[24] Our simulations suggest that 6-methylthiopurine is formed mainly in the N7 tautomer, though it could transform into the N9 tautomer in solution after leaving the active site.

Interestingly, from inspecting the trajectories of the 1 ns QM/MM MD simulations, the substrate orientations are different by a ~90° rotation in the molecular plane for N7 and N9 setups (Figure 6), which may be caused by the interactions between the different electrostatic potentials of the substrates and the microenvironments of the binding sites. As a result, for N9 setup, the product is formed in a *cis* conformation, while in *trans* for N7

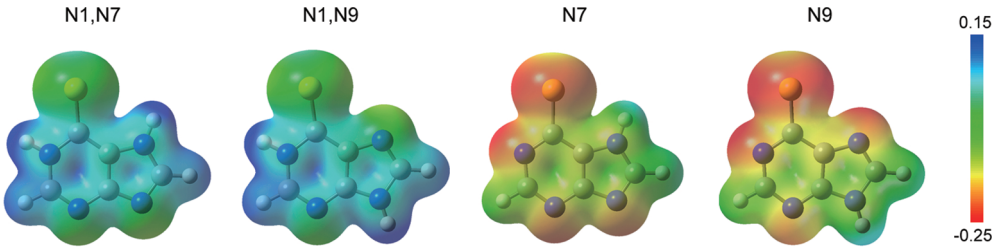

Figure 3. Electrostatic potential for different protonation states of 6-mercaptopurine mapped on the density isosurface (0.01e). The blue (red) color represents a positive (negative) potential. A large negative potential at S_ζ will facilitate nucleophilic attack.

Table 2. Statistics of Some Key Geometry Values during the 1 ns QM/MM MD Simulations

	$S_\zeta - C_\varepsilon$ (Å)	$S_\zeta - C_\varepsilon - S_\delta$ (deg)
N7	3.32 ± 0.22	149.5 ± 14.4
N9	3.48 ± 0.27	161.9 ± 8.1
N1,N7	3.32 ± 0.22	158.6 ± 10.8
N1,N9	3.44 ± 0.23	149.9 ± 11.6

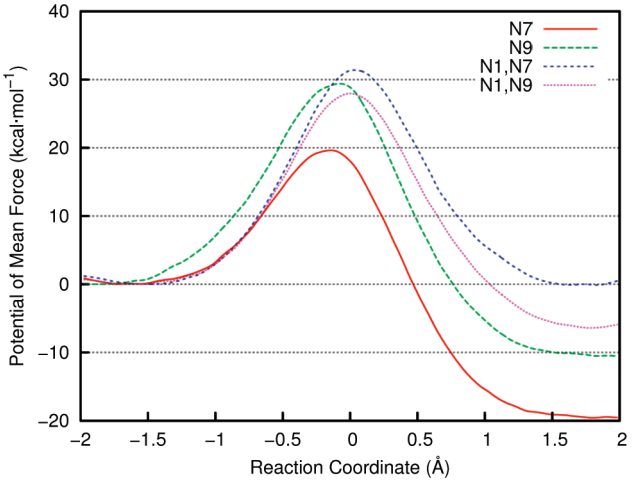

Figure 4. PMF along the putative reaction coordinate r which was defined as $r = d(S_\zeta - C_\varepsilon) - d(C_\varepsilon - S_\delta)$.

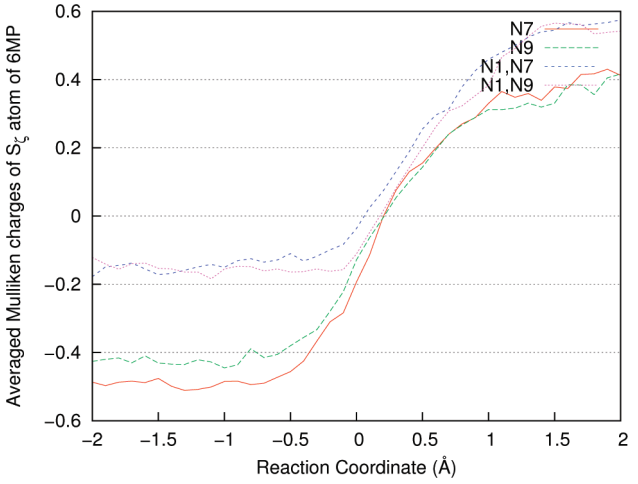

Figure 5. Mulliken charges of S_ζ atom of 6MP averaged in a bin width of 0.1 Å along the reaction coordinate.

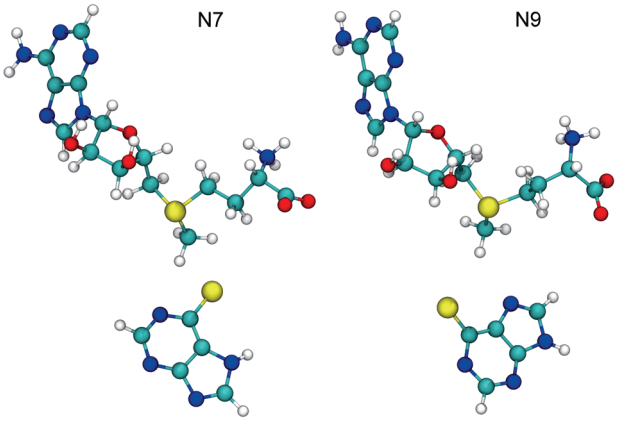

Figure 6. Relative positions of SAM and 6MP for N7 and N9 setups. For setup N9, the product is formed in *cis* conformation, while in *trans* for setup N7.

setup. The larger steric effect in the *cis* conformation may lead to a larger difference of the activation barriers between N7 and N9 setups.

Deprotonation of the Substrate. The MTase reaction mechanism requires a deprotonation step before, during, or after the methyl-transfer step. For TPMT, the enzyme–substrate crystal structures provide no good candidates of residues or solvent molecules for the substrate deprotonation. However, on the basis of the trajectories of the MD simulations, the internal solvent channel of the enzyme can provide a partial solvent access to the substrate. One of the two open ends of the channel, which can be seen as cavities on the surface of the enzyme, connects the substrate binding pocket through a water molecule which is hydrogen-bonded to 6MP. To analyze the behavior of the water molecules in the cavity, we calculated the spatial distribution function (SDF) of the water oxygen atoms based on the trajectory of the 1 ns QM/MM MD simulation of setup N1,N7 (see Figure 7). In this cavity, there are three water molecule sites with high occupancies, and it is interesting to found that the substrate is bridged with Asp23, which is highly conserved in the TPMT family, through a chain of these three water molecules. On the basis of this observation, we propose that the substrate is deprotonated by Asp23 through a water chain, and the protonated Asp23 which is on the surface of the enzyme can lose the proton to the solvent afterward. The water-mediated substrate deprotonations have also been observed in other MTases.[26–28]

dx.doi.org/10.1021/jp2027516 |*J. Phys. Chem. B* 2011, 115, 8033–8037

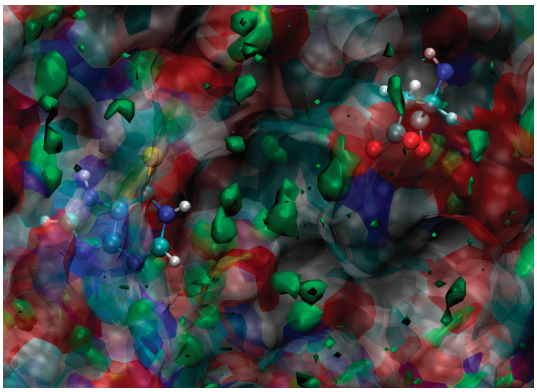

Figure 7. The 3.5 isosurface of the spatial distribution function of the water oxygen atoms (green solid surface). The protein is represented as a transparent surface, while 6MP and Asp23 are shown as the ball-and-stick model.

CONCLUSION

In this study, we have used QM/MM MD simulations and the umbrella sampling technique to investigate the reaction mechanism of the methylation of 6MP catalyzed by TPMT. Different system setups have been explored to find the favored binding orientations and protonation patterns of the substrate. Substrates can be positioned in an ideal NAC with the binding orientation as in chain A of the enzyme−substrate complex X-ray structure. The methyl-transfer step takes place in a classic S_N2 reaction mechanism after the deprotonation of the substrate. We highlight the conserved residue Asp23 responsible for the substrate deprotonation through a water chain in the internal solvent channel of the enzyme. The active tautomeric form of 6MP is N7 with a activation free energy barrier of 19.6 kcal/mol, which is in good agreement with the available experimental rate constant data.

AUTHOR INFORMATION

Corresponding Author

*E-mail: ljy121@jlu.edu.cn.

ACKNOWLEDGMENT

This work was supported by the National Natural Science Foundation of China (20973077), the Program for New Century Excellent Talents in University (NCET). The authors are grateful to the referees for their valuable comments on improving the manuscript.

REFERENCES

(1) Coulthard, S.; Hogarth, L. *Invest. New Drugs* **2005**, *23*, 523–532.
(2) Wang, L.; Weinshilboum, R. *Oncogene* **2006**, *25*, 1629–1638.
(3) Schubert, H. L.; Blumenthal, R. M.; Cheng, X. *Trends Biochem. Sci.* **2003**, *28*, 329–335.
(4) Wu, H.; Horton, J. R.; Battaile, K.; Allali-Hassani, A.; Martin, F.; Zeng, H.; Loppnau, P.; Vedadi, M.; Bochkarev, A.; Plotnikov, A. N.; Cheng, X. *Proteins* **2007**, *67*, 198–208.
(5) Peng, Y.; Feng, Q.; Wilk, D.; Adjei, A. A.; Salavaggione, O. E.; Weinshilboum, R. M.; Yee, V. C. *Biochemistry* **2008**, *47*, 6216–6225.
(6) Dolinsky, T. J.; Czodrowski, P.; Li, H.; Nielsen, J. E.; Jensen, J. H.; Klebe, G.; Baker, N. A. *Nucleic Acids Res.* **2007**, *35*, W522–W525.
(7) Dolinsky, T. J.; Nielsen, J. E.; McCammon, J. A.; Baker, N. A. *Nucleic Acids Res.* **2004**, *32*, W665–W667.
(8) Li, H.; Robertson, A. D.; Jensen, J. H. *Proteins* **2005**, *61*, 704–721.
(9) Case, D. A.; Darden, T. A.; Cheatham, T. E., III; Simmerling, C. L.; Wang, J.; Duke, R. E.; Luo, R.; Crowley, M.; Walker, R. C.; Zhang, W.; Merz, K. M.; Wang, B.; Hayik, S.; Roitberg, A.; Seabra, G.; Kolossváry, I.; Wong, K. F.; Paesani, F.; Vanicek, J.; Wu, X.; Brozell, S. R.; Steinbrecher, T.; Gohlke, H.; Yang, L.; Tan, C.; Mongan, J.; Hornak, V.; Cui, G.; Mathews, D. H.; Seetin, M. G.; Sagui, C.; Babin, V.; Kollman, P. A. *AMBER 10*; University of California:: San Francisco, 2008.
(10) Repasky, M. P.; Chandrasekhar, J.; Jorgensen, W. L. *J. Comput. Chem.* **2002**, *23*, 1601–1622.
(11) Tirado-Rives, J.; Jorgensen, W. L. *J. Chem. Theory Comput.* **2008**, *4*, 297–306.
(12) Cornell, W. D.; Cieplak, P.; Bayly, C. I.; Gould, I. R.; Merz, K. M.; Ferguson, D. M.; Spellmeyer, D. C.; Fox, T.; Caldwell, J. W.; Kollman, P. A. *J. Am. Chem. Soc.* **1995**, *117*, 5179–5197.
(13) Hornak, V.; Abel, R.; Okur, A.; Strockbine, B.; Roitberg, A.; Simmerling, C. *Proteins* **2006**, *65*, 712–725.
(14) Jorgensen, W. L.; Chandrasekhar, J.; Madura, J. D.; Impey, R. W.; Klein, M. L. *J. Chem. Phys.* **1983**, *79*, 926–935.
(15) Darden, T.; York, D.; Pedersen, L. *J. Chem. Phys.* **1993**, *98*, 10089–10092.
(16) Essmann, U.; Perera, L.; Berkowitz, M. L.; Darden, T.; Lee, H.; Pedersen, L. G. *J. Chem. Phys.* **1995**, *103*, 8577–8593.
(17) Ryckaert, J.; Ciccotti, G.; Berendsen, H. J. C. *J. Comput. Phys.* **1977**, *23*, 327–341.
(18) Kastner, J.; Thiel, W. *J. Chem. Phys.* **2005**, *123*, 144104.
(19) Kastner, J.; Thiel, W. *J. Chem. Phys.* **2006**, *124*, 234106.
(20) Becke, A. D. *J. Chem. Phys.* **1993**, *98*, 5648–5652.
(21) Lee, C.; Yang, W.; Parr, R. G. *Phys. Rev. B* **1988**, *37*, 785–789.
(22) Frisch, M. J.; Trucks, G. W.; Schlegel, H. B.; Scuseria, G. E.; Robb, M. A.; Cheeseman, J. R.; Scalmani, G.; Barone, V.; Mennucci, B.; Petersson, G. A.; Nakatsuji, H.; Caricato, M.; Li, X.; Hratchian, H. P.; Izmaylov, A. F.; Bloino, J.; Zheng, G.; Sonnenberg, J. L.; Hada, M.; Ehara, M.; Toyota, K.; Fukuda, R.; Hasegawa, J.; Ishida, M.; Nakajima, T.; Honda, Y.; Kitao, O.; Nakai, H.; Vreven, T.; Montgomery, J. A., Jr.; Peralta, J. E.; Ogliaro, F.; Bearpark, M.; Heyd, J. J.; Brothers, E.; Kudin, K. N.; Staroverov, V. N.; Kobayashi, R.; Normand, J.; Raghavachari, K.; Rendell, A.; Burant, J. C.; Iyengar, S. S.; Tomasi, J.; Cossi, M.; Rega, N.; Millam, N. J.; Klene, M.; Knox, J. E.; Cross, J. B.; Bakken, V.; Adamo, C.; Jaramillo, J.; Gomperts, R.; Stratmann, R. E.; Yazyev, O.; Austin, A. J.; Cammi, R.; Pomelli, C.; Ochterski, J. W.; Martin, R. L.; Morokuma, K.; Zakrzewski, V. G.; Voth, G. A.; Salvador, P.; Dannenberg, J. J.; Dapprich, S.; Daniels, A. D.; Farkas, Ö.; Foresman, J. B.; Ortiz, J. V.; Cioslowski, J.; Fox, D. J. *Gaussian 09, Revision A.02*; Gaussian, Inc.: Wallingford, CT, 2009.
(23) Pazderski, L.; Lakomska, I.; Wojtczak, A.; Szlyk, E.; Sitkowski, J.; Kozerski, L.; Kamienski, B.; Kozminski, W.; Tousek, J.; Marek, R. *J. Mol. Struct.* **2006**, *785*, 205–215.
(24) Chenon, M. T.; Pugmire, R. J.; Grant, D. M.; Panzica, R. P.; Townsend, L. B. *J. Am. Chem. Soc.* **1975**, *97*, 4636–4642.
(25) Krynetski, E. Y.; Krynetskaia, N. F.; Yanishevski, Y.; Evans, W. E. *Mol. Pharmacol.* **1995**, *47*, 1141–1147.
(26) Zhang, X.; Bruice, T. C. *Biochemistry* **2007**, *46*, 5505–5514.
(27) Zhang, X.; Bruice, T. C. *Biochemistry* **2007**, *46*, 9743–9751.
(28) Zhang, X.; Bruice, T. C. *Biochemistry* **2007**, *46*, 14838–14844.